Biophysical Chemistry 203–204 (2015) 12–21

Contents lists available at ScienceDirect

Biophysical Chemistry

journal homepage: http://www.elsevier.com/locate/biophyschem

Impact of molecular weight and degree of conjugation on the thermodynamics of DNA complexation and stability of polyethylenimine-graft-poly(ethylene glycol) copolymers

Ryan J. Smith, Rachel W. Beck, Lisa E. Prevette *

Department of Chemistry, University of St. Thomas, 2115 Summit Ave., St. Paul, MN 55105-1079, United States

HIGHLIGHTS

- Effect of PEGylation on DNA binding thermodynamics is quantified for the first time.
- Polyplex aggregation thermodynamics are quantified for the first time.
- Limitations of popular indirect DNA binding assays are revealed.
- PEGylation reduces affinity as a function of molecular weight and % conjugation.

GRAPHICAL ABSTRACT

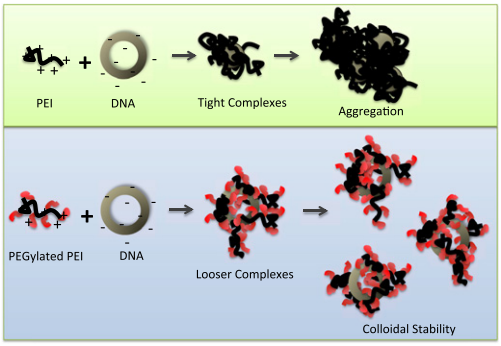

ARTICLE INFO

Article history:
Received 1 April 2015
Received in revised form 27 April 2015
Accepted 28 April 2015
Available online 7 May 2015

Keywords:
Polyethylenimine gene delivery
Poly(ethylene glycol) conjugation
DNA complexation
Isothermal titration calorimetry
Polyplex stability
DNA binding thermodynamics

ABSTRACT

Poly(ethylene glycol) (PEG) is often conjugated to polyethylenimine (PEI) to provide colloidal stability to PEI–DNA polyplexes and shield charge leading to toxicity. Here, a library of nine cationic copolymers was synthesized by grafting three molecular weights (750, 2000, 5000 Da) of PEG to linear PEI at three conjugation ratios. Using isothermal titration calorimetry, we have quantified the thermodynamics of the associations between the copolymers and DNA and determined the extent to which binding is hindered as a function of PEG molecular weight and conjugation ratio. Low conjugation ratios of 750 Da PEG to PEI resulted in little decrease in DNA affinity, but a significant decrease—up to two orders of magnitude—was found for the other copolymers. We identified limitations in determination of affinity using indirect assays (electrophoretic mobility shift and ethidium bromide exclusion) commonly used in the field. Dynamic light scattering of the DNA complexes at physiological ionic strength showed that PEI modifications that did not reduce DNA affinity also did not confer significant colloidal stability, a finding that was supported by calorimetric data on the aggregation process. These results quantify the DNA interaction thermodynamics of PEGylated polycations for the first time and indicate that there is an optimum PEG chain length and degree of substitution in the design of agents that have desirable properties for effective in vivo gene delivery.

1. Introduction

Gene-based therapies have potential to treat many acquired and inherited disorders, such as cancers, blindness, blood diseases, deafness, Parkinson's disease, X-SCID, sickle cell anemia, and cystic fibrosis [1–8].

* Corresponding author. Tel.: +1 651 962 5672; fax: +1 651 962 5201.
E-mail address: lisa.prevette@stthomas.edu (L.E. Prevette).

http://dx.doi.org/10.1016/j.bpc.2015.04.005
0301-4622/

Cationic polymers, such as polyamidoamine dendrimer, poly-L-lysine, and polyethylenimine, have been shown to complex nucleic acids, have effective cell transfection properties, and are easily modified [9–11]. A major hurdle in the development of a viable gene therapy system, however, has been the effectiveness of the nucleic acid delivery in vivo. There are many undesirable side effects of current nonviral delivery agents, such as cytotoxicity, nonspecific cellular uptake and complement activation by the host's immune system, which leads to poor blood circulation time (Zhang, Satterlee and Huang provide a nice review [12]).

Polyethylenimine (PEI) is one of the most effective nonviral gene delivery vectors [9,13]. Previous research has shown that complexation by PEI protects the nucleic acid against enzymatic degradation and aids in endosomal escape via what has been dubbed the "proton sponge hypothesis [13–15]." The latter characteristic is a result of PEI's buffer capacity through its many amines, which have a range of pK_as to absorb protons as the pH drops to about 6 in early endosomes, 5.5 in late endosomes and 5 in lysosomes [16,17]. However, PEI can be cytotoxic, permeabilizing the cell plasma membrane, which is a function of its charge density [18–20]. In addition, PEI/DNA complexes (referred to as polyplexes) are susceptible to nonspecific cell uptake and targeting by the reticuloendothelial system (RES) when they aggregate at physiological ionic strength [21–25], and as a result, exhibit short circulation time in vivo [25–27].

To improve colloidal stability and biocompatibility, polyethylene glycol (PEG) is often grafted to PEI [26,28–34]. Since PEG is a neutral, hydrophilic molecule, it shields the PEI/DNA polyplex positive surface charge and provides steric hindrance to flocculation in physiological media [23,25,27,32–34]. Usually longer PEG chains are necessary; however, at high conjugation ratios, relatively short 350 Da PEG were effective at preventing PEI polyplex aggregation at physiological ionic strength [23]. *In vivo* experiments in mice showed improved circulation time of PEI/DNA polyplexes as a result of PEGylation [25,27]. Many groups have studied the biological properties of block copolymers of 25 kDa branched PEI and linear PEG as a function of amount of grafting and PEG molecular weight [23,25,27,31,33,34]. Cytotoxicity was reduced as a function of the amount of PEG grafting, but independent of PEG chain length, in 3T3 mouse fibroblast and human cervix epithelial carcinoma cells [31,34]. These results suggest that reducing the charge density of the PEI amines is more important than steric hindrance for biocompatibility of these agents. However, Sung et al. found that both PEG conjugation ratio and molecular weight affect cytotoxicity of PEI in C3 tumor cells, with higher total PEG mass per PEI reducing deleterious effects [23]. Unfortunately, the in vitro transfection efficiency of many of these polyplexes was compromised by PEGylation [23,31,34]. These results demonstrate that there is a delicate balance between PEG molecular weight and degree of grafting for optimal biological properties of these gene delivery agents.

Although the addition of PEG chains enhances stability and biocompatibility, it also likely affects PEI's ability to complex DNA. A few groups have shown indirect evidence of weaker association with PEGylated PEI through exclusion of a DNA intercalator or gel retardation assays [23,33]. A study conducted by Luo et al. is the only one known where the effect of PEG molecular weight and conjugation ratio on PEI polyplex stability was investigated thoroughly [32]. All PEGylated branched PEIs protected bound DNA from degradation by DNase I. A heparin displacement assay was also performed which showed that all PEI complexes were susceptible to competitive release of bound DNA and that complexes formed using PEI copolymers with 50% PEG by weight were especially reversible. These reports warrant a deeper understanding of interaction energetics.

This study herein presents a quantitative investigation of how PEG molecular weight and conjugation ratio affect not only the thermodynamics of the complexation of DNA by PEI but also the tendency of PEI/DNA polyplexes to aggregate. A library of nine copolymers was synthesized with commonly used commercially available PEGs of 750, 2000 and 5000 Da conjugated from low to high degrees of substitution (Fig. 1), which reflect a range that is both relevant to biological data in the literature and likely to reveal differences in function. Amine coupling through N-hydroxysuccinimide-activated ester was selected for its ease and efficiency and, hence, popularity for PEG conjugation. Then, the DNA affinity of each polymer was investigated through ethidium bromide exclusion assays (EBEA), electrophoretic mobility shift assays (EMSA), and isothermal titration calorimetry (ITC). Dynamic light scattering (DLS) characterized the colloidal stability of the polyplexes in physiological conditions, which was further supported by quantitative calorimetry data. The conclusions of this research reveal disadvantages of using common, indirect assays to compare DNA affinity and provide a detailed thermodynamic explanation of the biological efficacy of PEGylated PEI gene delivery agents.

2. Materials and methods

O-[(*N*-Succinimidyl)succinyl-aminoethyl]-*O*′-methylpolyethylene glycol 750, 2000 and 5000 Da MW [PEG(750), PEG(2000) and PEG (5000), respectively] and phosphate buffered saline (PBS) were purchased from Sigma Aldrich (St. Louis, MO) and used without further purification. Linear polyethylenimine, MW 25 kDa (Polysciences, Inc.; Warrington, PA) was solubilized in water by the addition of 0.1 M HCl and stirred for 48 h. Sodium hydroxide was then added to return the pH to 7.4. To remove low molecular weight impurities, dialysis was performed using 8–10 kDa MWCO Spectra/Por cellulose tubing (Spectrum Laboratories, Inc.; Rancho Dominguez, CA) against nanopure water with five water changes over a period of 48 h and the final product was lyophilized. Technical-grade 3546 bp plasmid DNA with a CMV promoter was purchased from PlasmidFactory (Bielefeld, Germany). SYBR® Green I nucleic acid gel stain was from Life Technologies; Carlsbad, CA. 2,7-Diamino-10-ethyl-9-phenyl-phenanthridinium bromide (95%) was purchased from Sigma Aldrich (St. Louis, MO). Deuterium Oxide (99.9%) was purchased from Cambridge Isotope Laboratories, Inc. (Anderover, MA). Genetic technology grade agarose was purchased from MP Biomedicals, LLC (Solon, OH).

2.1. Conjugation of PEG

Purified PEI was dissolved in 2 mL of 10 mM phosphate buffer pH 8. The same volume of PEG solution in the same buffer was added dropwise to the PEI with vigorous stirring, and the mixture was allowed to react for 24 h at room temperature. The product was then dialyzed extensively against nanopure water and lyophilized. This procedure was completed as described for all nine copolymers with molar feeding

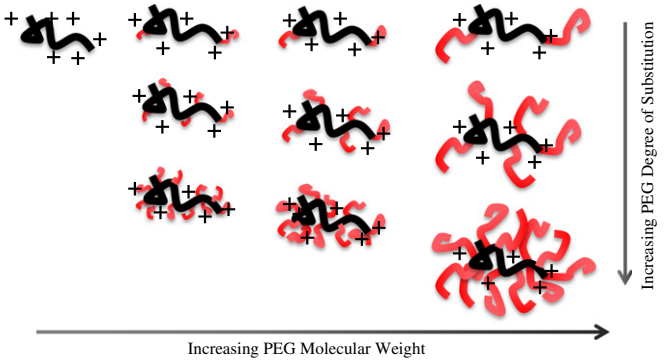

Fig. 1. The series of PEG-*g*-PEI copolymers synthesized to study the effect of increasing PEG molecular weight and degree of substitution on the DNA affinity and colloidal stability of the polyplexes.

ratios of 1:3, 1:12, and 1:30 PEG:PEI amine. Each product was characterized via ^{1}H and $^{1}H-^{13}C$ HSQC NMR. The results were used to correct the number of protonatable amines per repeat unit of PEI, and this corrected number was used to determine all N/P ratios used throughout the DNA binding and flocculation studies.

2.2. Ethidium bromide exclusion assay

The decrease in fluorescence of DNA-intercalated ethidium upon polymer binding was used to compare the relative DNA binding affinities of the polymers, according to the method of Read et al. [35]. A Horiba Fluoromax spectrophotometer was used to record fluorescence under the following data acquisition parameters: λ_{ex} = 510 nm, λ_{em} = 588 nm, slit width = 10 nm, integration time of 3 s, and an acquisition mode = S/R. All solutions were made in 10 mM phosphate buffer, pH 7.4. A 1.000 mL aliquot of an 800 μg/mL solution of ethidium bromide (EtBr) was mixed with 1.000 mL of 1.0 μg/mL DNA in a 1-cm pathlength quartz cuvette. Titrations of DNA were performed with each polymer in 50.0 μL aliquots to reach an N/P ratio (moles of polymer amine/moles of DNA phosphate) of 6. After each addition of polymer, the solution was gently mixed, and the reduced fluorescence (F) was measured. This procedure was performed in triplicate for each of the nine copolymers as well as unconjugated PEI. The relative fluorescence was determined using Eq. (1):

$$\text{relative}\,fluorescence = \frac{F - F_{bg}}{F_{DNA} - F_{bg}} \tag{1}$$

where F_{bg} is the background fluorescence of free ethidium in buffer and F_{DNA} is the fluorescence of ethidium–DNA complex before addition of polycation.

2.3. Electrophoretic mobility shift assay

Polyplexes were formed by adding an equal volume of polymer solution to 10.0 μL of 20 μg/mL pDNA solution, both in DNase-/RNase-free water, to result in N/P ratios of 0–30. The two solutions were mixed well for each ratio and incubated at room temperature for 20 min. To each well of a 0.6% agarose gel, 10 μL of polyplex sample mixed with loading dye was added. The gel was run at 60 V for approximately 50 min in 1× TAE buffer. Afterward, the gel was stained with SYBR® Green in water for 30 min, followed by 5 min destaining.

2.4. Isothermal titration calorimetry

Binding thermodynamic parameters were obtained with a NanoITC (TA Instruments; Newcastle, DE) at 25 °C. All solutions were in 10 mM HEPES buffer at pH 7.4 and degassed prior to injection. A 0.50–1.2 mM polymer solution was titrated into 0.996 mL of 0.10 mM DNA solution using 10 μL injections with a 300 s spacing between to allow equilibration. The heat of dilution of the polymer was obtained by averaging the last few injections and subtracting this heat from each peak in the titration. The magnitude of this dilution heat was identical to that found through performing a control titration of polymer into buffer (data not shown). A similar control experiment of buffer into DNA solution was performed, and its dilution heat was found to be negligible. The data was fit to a standard Multiple Site model using Nanoanalyze software, with the enthalpy (ΔH), binding constant (K), and stoichiometry (n) as free-floating parameters. Eq. (2) describes the experimental measurement

$$\Delta Q_i = Q_i + \frac{dV_i}{V_o}\left[\frac{Q_i + Q_{i-1}}{2}\right] - Q_{i-1} \tag{2}$$

where ΔQ_i is the heat absorbed or released as a result of the i^{th} injection, V_o is the active cell volume, and dV_i is the change in volume due to the injection. The total heat content Q_i is related to the thermodynamic parameters using Eq. (3):

$$Q_i = n\Theta_i M \Delta H V_o \tag{3}$$

where n is the number of sites, ΔH is the change in enthalpy, Θ_i is the ratio of sites occupied by ligand X after the i^{th} injection, and M is the bulk concentration of macromolecule in V_o. Solving for Θ_i provides Eq. (4):

$$Q_i = \frac{nM\Delta H V_o}{2}\left[1 + \frac{X}{nM} + \frac{1}{nKM} - \sqrt{\left(1 + \frac{X}{nM} + \frac{1}{nKM}\right)^2 - \frac{4X}{nM}}\right] \tag{4}$$

where X is the bulk concentration of ligand, and K is the association constant. The Multiple Site model is an extension of the Independent model above where a second set of thermodynamic parameters adds to the total heat content Q, as in Eq. (5):

$$Q = M_t V_o (n_1 \Theta_1 \Delta H_1 + n_2 \Theta_2 \Delta H_2). \tag{5}$$

The PEI–DNA interaction was also studied in different buffers of the same ionic strength to determine the intrinsic binding enthalpy and the number of protons taken up by PEI upon binding. The chosen buffers were 3-morpholino-2-hydroxypropanesulfonic acid (MOPSO) and 2-amino-2-(hydroxymethyl)-1,3-propanediol (Tris) and 4-(2-hydroxyethyl)piperazine-1-ethanesulfonic acid (HEPES) with ionization enthalpies of 25.0, 47.5 and 20.4 kJ/mol, respectively at 25 °C [36].

2.5. Dynamic light scattering

PEI polyplexes were formed at N/P = 6 using 150.0 μL of polymer and 150.0 μL of 0.040 mg/μL DNA both in DNase-/RNase-free water. The polyplexes were incubated at room temperature for 20 min before being diluted with 700.0 μL of water or 1× PBS. The hydrodynamic diameters were measured after 0, 40, 80, and 120 min at 37 °C on a Malvern Zetasizer Nano ZS (Worchestershire, UK) with a 4 mW He–Ne laser operating at 633 nm with a 173° scattering angle. Three separately prepared polyplex samples were measured (diameters reported as the z-average), then averaged and the standard deviations reported.

3. Results

3.1. Characterization of copolymers

A series of PEI copolymers with a range of amine conjugation ratios of PEG(750), PEG(2000) and PEG(5000) was synthesized through different molar feeding ratios of the two components to obtain a library of increasing PEG content. Each product was characterized with 1D ^{1}H and 2D $^{1}H-^{13}C$ HSQC NMR spectroscopy. Due to the large molecular weight of the polymers (and hence, slow tumbling rate on the NMR timescale), broad, overlapping peaks were observed in all spectra. Integration of the PEG methoxy peak against the PEG methylene peak (Fig. 2, A and B, respectively) provided the accurate degrees of polymerization for the commercially available polyethylene glycols. These numbers were used to determine the molecular weight of each copolymer. To determine degrees of PEG substitution on PEI, integration of the PEG methoxy peak against the PEI methylene peak (Fig. 2, A and D, respectively) was used. For the PEG(750) copolymers, the PEG methoxy peak was overlaid with that of two of the PEG methylene protons on the end of the chain (clearly represented by the triplet at 3.22 ppm in Fig. 2 and confirmed by HSQC spectra, Supplemental Information Fig. S2 and S3); therefore, this peak was integrated to five protons. The feeding ratios of the conjugation reactions and resulting degrees of PEG substitution are presented in Table 1.

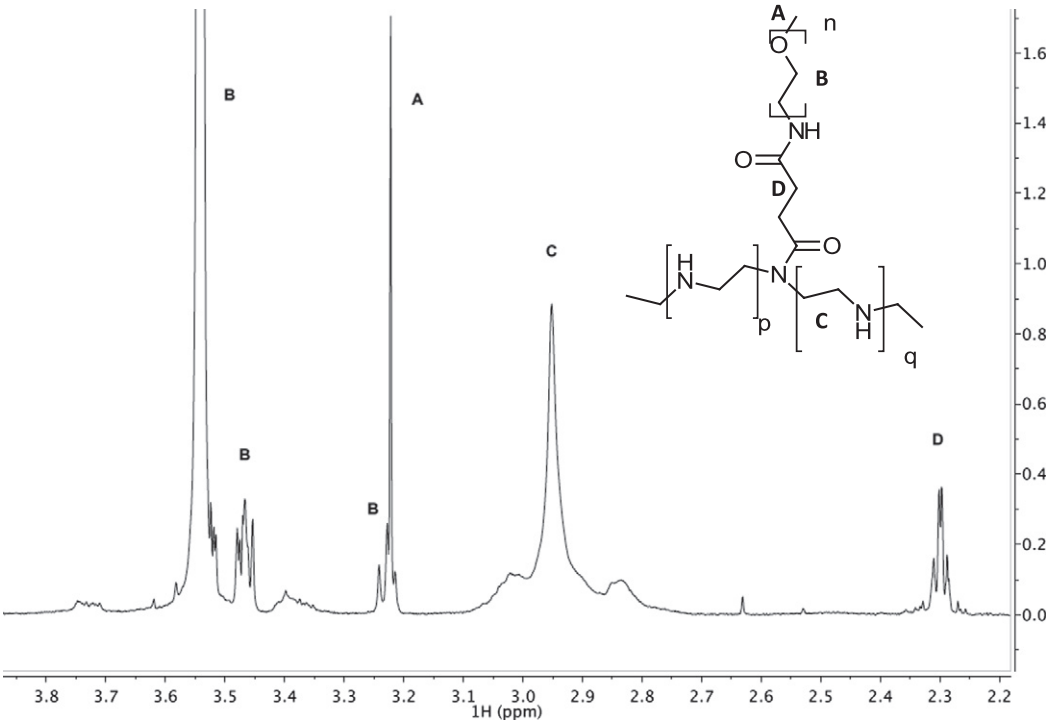

Fig. 2. ^{1}H NMR spectrum of PEI-*g*-PEG(750)$_{13}$ in D_2O.

3.2. Electrophoretic mobility shift assay

The well in which DNA migration was prevented represents the N/P ratio at which DNA is fully complexed to our polymer and the overall charge of the polyplex is neutral. Thus, this N/P ratio reflects polyplex stoichiometry. Fig. 3 contains the gel images from EMSA of unconjugated PEI (a) and PEI-*g*-PEG(5000)$_{5.5}$ (b). Table 2 displays this average N/P ratio for each polymer as determined by EMSA performed in triplicate. Some copolymers exhibited partial DNA binding, indicated by smearing of the bands. In these cases, the stoichiometric N/P ratio was taken as that where all of the nucleic acid was retained in the loading well. Preferential binding of the copolymers to the supercoiled fraction of the plasmid DNA was observed, as indicated by the disappearance of the band with the most mobility first. All PEGylated PEIs showed higher stoichiometries compared to unconjugated PEI, as expected due to steric hindrance. It can be noted that the 1:30 conjugation series had the lowest observed stoichiometries (only slightly higher than that of unconjugated PEI), while the 1:3 series was in general found to have the highest stoichiometries, suggesting weaker DNA binding with increasing degree of substitution. A trend of increasing N/P ratio with increasing PEG molecular weight was observed within the 1:30 and 1:12 conjugation series, as expected. However, the trend was not as clear for the most PEGylated 1:3 series.

Table 1
Composition of PEI-*g*-PEG copolymers.

Copolymer	Feeding ratio (moles PEG:moles PEI N)	Product ratio (moles PEG:moles PEI N)	Degree of substitution (%)
PEI-*g*-PEG(750)$_{13}$	1:3	1:8	13
PEI-*g*-PEG(750)$_{5.0}$	1:12	1:20	5.0
PEI-*g*-PEG(750)$_{3.2}$	1:30	1:31	3.2
PEI-*g*-PEG(2000)$_{25}$	1:3	1:4	25
PEI-*g*-PEG(2000)$_{5.0}$	1:12	1:20	5.0
PEI-*g*-PEG(2000)$_{3.3}$	1:30	1:30	3.3
PEI-*g*-PEG(5000)$_{20}$	1:3	1:5	20
PEI-*g*-PEG(5000)$_{5.5}$	1:12	1:18	5.5
PEI-*g*-PEG(5000)$_{2.6}$	1:30	1:38	2.6

3.3. Ethidium bromide exclusion assays

DNA-intercalated ethidium cation is displaced as polycation binds the nucleic acid. Since water quenches the ethidium fluorescence, a decrease in intensity is seen as a function of increasing polymer concentration or N/P ratio. The fluorescence intensity of each titration point was normalized to that of N/P = 0 (free DNA) and the titration curves are plotted in Fig. 4 below. The half maximal inhibitory concentration (IC_{50}) of each polymer was found, and the corresponding N/P ratio was recorded. Most of the copolymers exhibited similar IC_{50} values to unconjugated PEI, however it can be noted that the average IC_{50} value of the 1:30 series is lower than the average IC_{50} value of the 1:12 series. Only the most PEGylated copolymers, PEI-*g*-PEG(2000)$_{25}$ and PEI-*g*-PEG(5000)$_{20,}$ showed significantly larger IC_{50} values. These titration curves mimicked those of adding PEG or buffer to DNA, suggesting that there was no interaction for these two copolymers, according to this assay. Table 3 displays the IC_{50} values of the entire polymer library.

3.4. Isothermal titration calorimetry

Nonlinear least squares regression analysis of each polymer–DNA thermogram to the Independent (Eq. (3)) and Multiple Site (Eq. (5)) models was performed. The Independent model, corresponding to a singular binding event, provided a poor fit to the data; therefore the binding thermodynamic parameters, K_1, ΔH_1, n_1, K_2, $\Delta H2$, and n_2 (for Site 1 and Site 2, respectively) of each polymer to DNA were determined by fitting all thermograms to the Multiple Site model and averaging at least three independent titrations. An example thermogram and fit is shown in Fig. 5 for PEI-*g*-PEG(5000)$_{5.5}$. The Site 1 interaction is exothermic for unconjugated PEI and all copolymers, and the stoichiometries range from N/P = 0.33 to N/P = 1.7. The association constant for this site (K_1) for all copolymers, ranging from 5.4×10^6 to 5.4×10^8 M^{-1}, is smaller than that for unconjugated PEI (7.6×10^8 M^{-1}). The Site 2 interaction is endothermic for all polymers and the stoichiometries are all

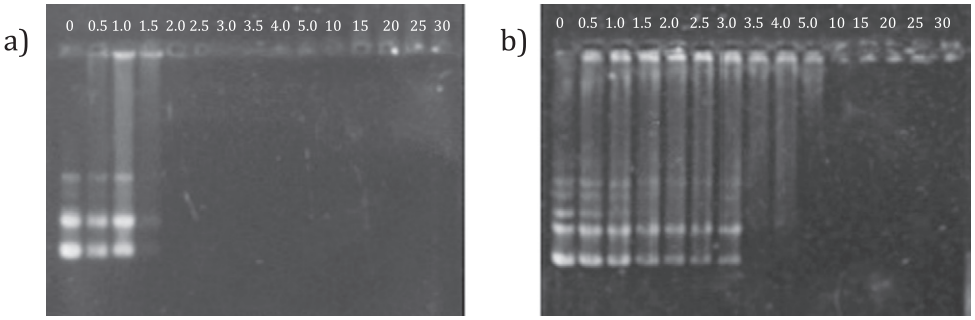

Fig. 3. Electrophoretic mobility shift assay, as a function of N/P ratio, in agarose gel for DNA complexes of a) unconjugated PEI and b) PEI-*g*-PEG(5000)$_{5.5}$.

between N/P = 0.10 and N/P = 0.40. The similarity of n_2 values suggests that the Site 2 interaction is not very structurally dependent. The K_2 values vary, however, ranging from 4.4×10^4 to 2.2×10^7 M^{-1}, showing a significant decrease with copolymer PEG content. Fig. 6 graphically compares the average K_1 and K_2 values for the interaction of each polymer with DNA. Binding entropies were calculated for each copolymer from the K and ΔH values, and the enthalpy–entropy compensation for each interaction is shown in Fig. 7. Based on the fit parameters, Site 1 is attributed to electrostatic polymer amine–DNA phosphate binding, and Site 2 is aggregation of charge neutral polyplexes, as described in more detail below.

The unconjugated PEI–DNA interaction was studied in different buffers. The association constants did not change significantly, but the observed binding enthalpy did. The relationship between the heat of ionization of the buffer, ΔH_{ion}, and the enthalpy of interaction, ΔH_{obs}, was linear, as shown in Fig. 8. The slope of the best-fit line provides the fraction of PEI amines taking up protons upon binding DNA and was found to be 0.28. The y-intercept of the line, −8.7 kJ/mol, provides the intrinsic heat of binding, independent of buffer effects.

3.5. Dynamic light scattering

The average hydrodynamic diameter of the polyplexes formed at N/P = 6 was measured in water (data not shown) and PBS (Fig. 9) over the course of 2 h. Polyplexes formed with unconjugated PEI are roughly 275 nm and remain that size in water but aggregate in conditions of physiological ionic strength to particles over 1 μm in hydrodynamic diameter. PEGylation prevents aggregation of PEI/DNA polyplexes as a function of PEG molecular weight and conjugation ratio. As shown in Fig. 9, copolymers with the shortest PEG chains [PEI-*g*-PEG(750)$_{3.2}$ and PEI-*g*-PEG(750)$_{5.0}$] form polyplexes that flocculate over time to the same size as those of unconjugated PEI, while copolymers with higher PEG content, even the 750 Da PEG when at high degree of substitution, form colloidally stable polyplexes.

Table 2
The average N/P ratio of the EMSA well in which DNA ceases to migrate.

Copolymer	N/P ratio
PEI	2.0
PEI-*g*-PEG(750)$_{13}$	9.0
PEI-*g*-PEG(2000)$_{25}$	4.0
PEI-*g*-PEG(5000)$_{20}$	9.0
PEI-*g*-PEG(750)$_{5.0}$	2.5
PEI-*g*-PEG(2000)$_{5.0}$	5.0
PEI-*g*-PEG(5000)$_{5.5}$	10
PEI-*g*-PEG(750)$_{3.2}$	2.5
PEI-*g*-PEG(2000)$_{3.3}$	3.0
PEI-*g*-PEG(5000)$_{2.6}$	3.0

4. Discussion

There is an abundance of empirical data on the effect of PEGylation on the transfection efficiency and cytotoxicity of polyethylenimine; however the conclusions are conflicting. Much of the confusion seems to be attributable to the way in which the agents are compared. For example, many authors use equal mass of each, in which case PEI with higher conjugation ratios or higher PEG molecular weight provides a lower concentration of protonatable amines. One would expect such copolymers to demonstrate lower cytotoxicity and lower cellular uptake, due to decreased charge density of the delivery agent, and this has been shown.

Fitzsimmons et al. was the first to point out the difference between comparing PEGylated PEIs of equal mass versus equal amine content [37]. The authors showed that when polyplex N/P ratios were corrected for amine content, the cytotoxicity in two cell lines was comparable throughout conjugation ratio and less difference in transfection efficiency was seen amongst the agents. Many groups hypothesize that low transfection efficiency of PEGylated PEIs is due to weaker/reversible DNA binding [34], so an understanding of copolymer–DNA thermodynamics is needed to explain biological efficacy. Thus, we completed a detailed analysis of the DNA binding affinity of a representative library of PEI–PEG copolymers of varying PEG molecular weight and degree of substitution through common qualitative studies used in the field of gene delivery, such as electrophoretic mobility shift and ethidium bromide exclusion assays, and quantitative thermodynamic studies through isothermal titration calorimetry, comparing all polymers through amine content.

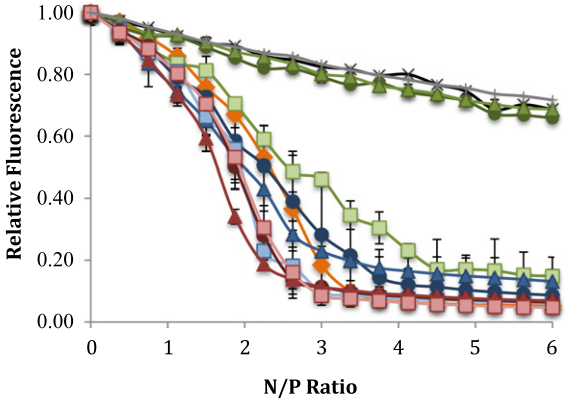

Fig. 4. Relative fluorescence of DNA–ethidium complexes titrated to increasing N/P ratios with PEI-*g*-PEG(750)$_{3.2}$ (□), PEG(2000)$_{3.3}$ (▲), PEI-*g*-PEG(5000)$_{2.6}$ (●), PEI-*g*-PEG(750)$_{5.0}$ (□), PEI-*g*-PEI-*g*-PEG(2000)$_{5.0}$ (▲), PEI-*g*-PEG(5000)$_{5.5}$ (●), PEI-*g*-PEG(750)$_{13}$ (□), PEI-*g*-PEG(2000)$_{25}$ (▲), PEI-*g*-PEG(5000)$_{20}$ (●), unmodified PEI (◆), PEG(5000) (×), buffer (+).

Table 3
Ethidium bromide exclusion assay IC_{50} values for polymer–DNA interactions.

Polymer	IC_{50} (N/P ratio)
PEI	2.5
PEI-*g*-PEG(750)$_{13}$	2.8
PEI-*g*-PEG(2000)$_{25}$	>6.0
PEI-*g*-PEG(5000)$_{20}$	>6.0
PEI-*g*-PEG(750)$_{5.0}$	2.1
PEI-*g*-PEG(2000)$_{5.0}$	2.2
PEI-*g*-PEG(5000)$_{5.5}$	2.0
PEI-*g*-PEG(750)$_{3.2}$	2.0
PEI-*g*-PEG(2000)$_{3.3}$	1.8
PEI-*g*-PEG(5000)$_{2.6}$	1.0

The different experiments herein all reveal DNA binding affinity but in various ways. Electrophoretic mobility shift assays use lack of DNA migration in an electric field to represent association via charge neutralization and increased complex mass. The output is information about the complex stoichiometry. In Fig. 3 and Table 2, we report the complex formulation ratio as an N/P ratio, where PEG-conjugated amines have been excluded, since the resultant amides are not protonatable ($pK_a = -0.5$). EMSA results showed that all PEGylated copolymers form DNA complexes with higher N/P stoichiometries than unconjugated PEI. This means more polymer amine was needed to neutralize the DNA phosphate backbone, suggesting inaccessibility due to steric hindrance. Petersen et al. showed the same result for PEGylated branched PEIs [31].

According to our EMSA results, increasing either PEG molecular weight or conjugation ratio negatively affected PEI–DNA complex formation. The PEG chain length trend is generally clear. We saw no difference between PEI-*g*-PEG(2000)$_{3.3}$ and PEI-*g*-PEG(5000)$_{2.6}$ but that is likely due to the fact that there are slightly less PEG chains on the PEI-*g*-PEG(5000)$_{2.6}$. Similarly, Zhang et al. found that PEI-*g*-PEG(2000) bound DNA more efficiently than PEI-*g*-PEG(5000) at the same 0.3% ratio [34]. In terms of conjugation ratio, we noticed a threshold of PEG content where the difference in binding stoichiometry was detectable. There was a large jump in N/P from PEI-*g*-PEG(5000)$_{2.6}$ to PEI-*g*-PEG(5000)$_{5.5}$, but no change in N/P for the PEG(750) series until the highest degree of substitution. Zhang et al. showed similar thresholds with PEG(2000) and PEG(5000) on branched PEI [34]. The ratios at which these differences are significant reflect large increases in copolymer molecular weight, which would affect gel electrophoresis migration. Petersen et al. saw no effect of PEG(5000) conjugation ratio on DNA agarose gel mobility, but they only compared copolymers with up to 3% substitution of the PEI amines [31]. They were under the threshold of PEG content at which EMSA reveals differences in complex stoichiometry. These results suggest some limitations to this method of DNA binding analysis for PEGylated agents.

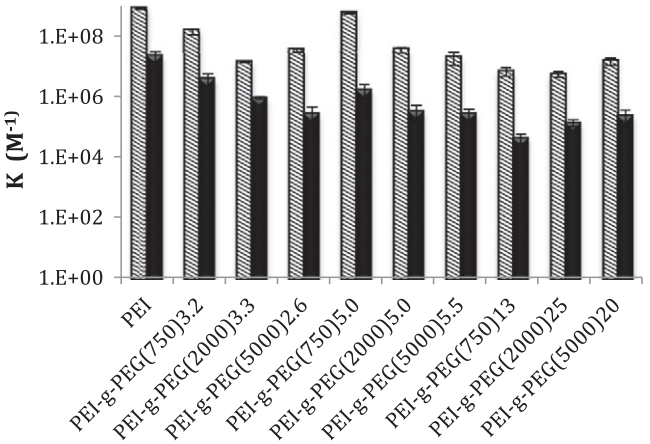

Fig. 6. The average K_1 (striped) and K_2 (solid) values of each copolymer/DNA binding interaction, as determined by ITC.

Ethidium bromide exclusion assays reveal DNA affinity through decreased fluorescence of the dye as it is sterically or electrostatically displaced from its intercalated state to free in solution, as PEI interacts. This is a commonly used assay for characterizing polyplex formation of nonviral gene delivery agents. Here, our results show that the most PEGylated PEIs (PEI-*g*-PEG(2000)$_{25}$ and PEI-*g*-PEG(5000)$_{20}$) are unable to displace ethidium from its intercalated state, with titrations curves similar to those of DNA-ethidium with unconjugated PEG or buffer (Fig. 4). This indicates that high PEG content in the copolymer significantly reduces DNA affinity. In fact, EBEA reports no DNA interaction for PEI-*g*-PEG(2000)$_{25}$ and PEI-*g*-PEG(5000)$_{20}$. We also saw statistically insignificant differences in DNA binding affinity amongst the seven least PEGylated copolymers, as did Maurstad et al. for a PEGylated chitosan series [38]. Thus, we conclude that this particular assay is not sensitive enough to probe the variations in binding seen with these gene delivery systems and with very weak associations, may provide false negative results.

The cause could be attributed to the nature of EBEA, in that it monitors DNA compaction rather than the electrostatic interaction directly. It is also important to note that intercalation of the ethidium cation may affect the interaction of the copolymers, due to induced DNA conformational changes (lengthening, unwinding and base pair tilting) [39–41] and partial DNA charge neutralization. Fant et al. thoroughly studied the use of ethidium for investigating DNA–polymer complexation [42]. They found that PEGylating a generation 5 polyamidoamine dendrimer did not affect the accessibility of DNA for ethidium, which renders our method valid for comparing across PEG molecular weights and conjugation ratios. They also showed a 10-fold decrease in the ethidium–DNA

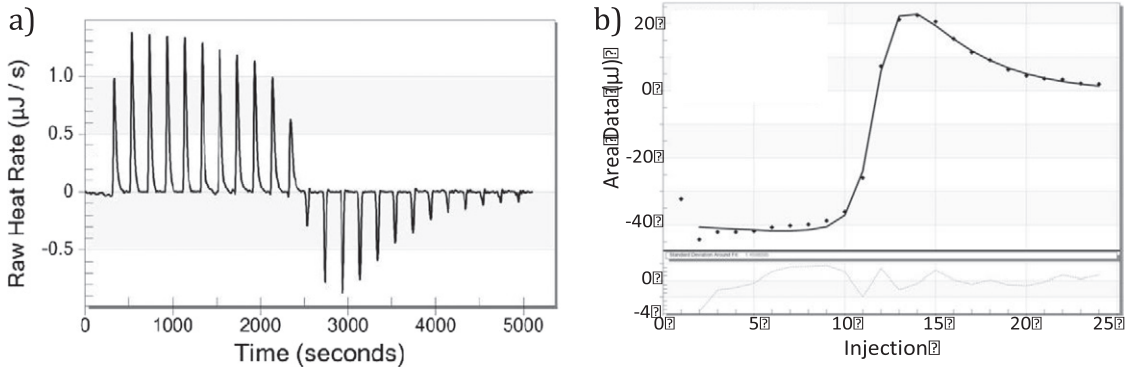

Fig. 5. a) ITC thermogram of PEI-*g*-PEG(750)$_{13}$ titrated into DNA in 10 mM HEPES buffer pH 7.4 at 25 °C. b) Integrated heat signal of thermogram fit with Multiple Site model and residuals.

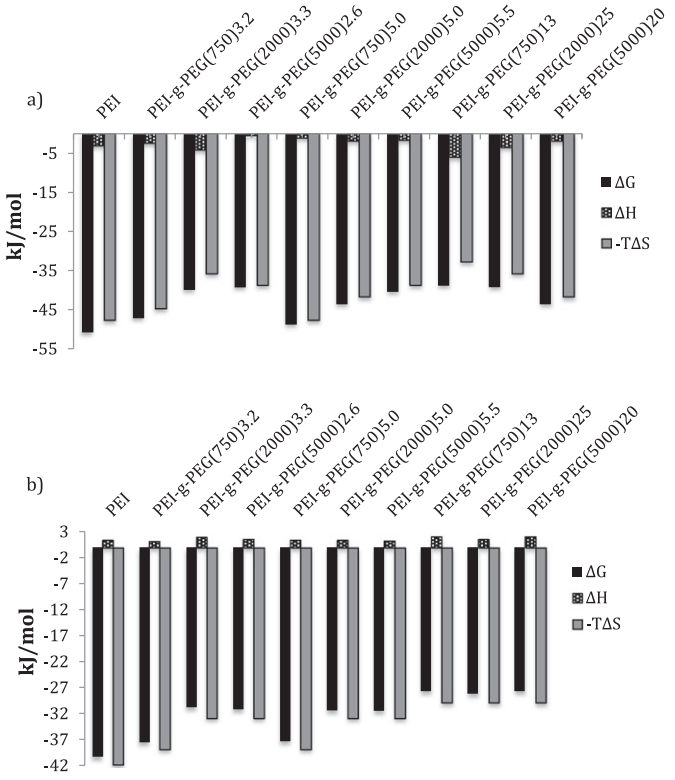

Fig. 7. Enthalpy and entropy contributions to the free energy of a) Site 1 and b) Site 2 associations at 25 °C.

binding constant with PEGylation of the dendrimer, suggesting that PEGylation leads to a more reversible DNA interaction. In support, we did notice differences in the total ethidium displaced from the polyplexes at the end of the titrations. At the higher PEG degrees of substitution, the fluorescence saturates at a higher intensity (see Fig. 4), suggesting that these copolymers are not able to condense the DNA to the same extent as unconjugated PEI. Although the assay was performed differently (adding ethidium to preformed polyplexes), Fant et al. saw evidence of looser complexation between DNA and dendrimer PEGylated at 20% degree of substitution [42]. This result is consistent with that of our similarly PEGylated PEI-*g*-PEG(2000)$_{25}$ and PEI-*g*-PEG(5000)$_{20}$, although the difference between unconjugated and PEGylated polymer is more pronounced in our studies, perhaps due to the traditional ethidium exclusion procedure or to the linear architecture of PEI leading to different binding mechanism than branched PAMAM dendrimer. In the study by Petersen et al., PEGylating branched PEI at high conjugation ratios led to larger, less spherical polyplexes, reflecting less DNA condensation [31].

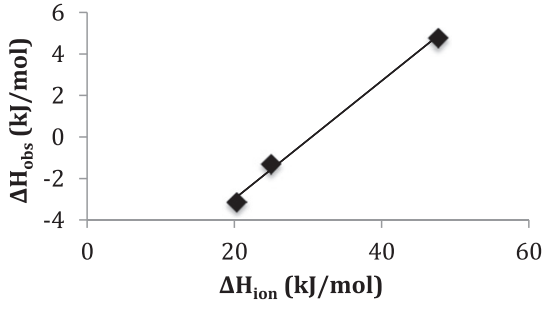

Fig. 8. Observed binding enthalpy (ΔH_{obs}) versus buffer ionization enthalpy (ΔH_{ion}; HEPES 20.4 kJ/mol, MOPSO 25.0 kJ/mol and Tris 47.5 kJ/mol) for the unconjugated PEI–DNA interaction.

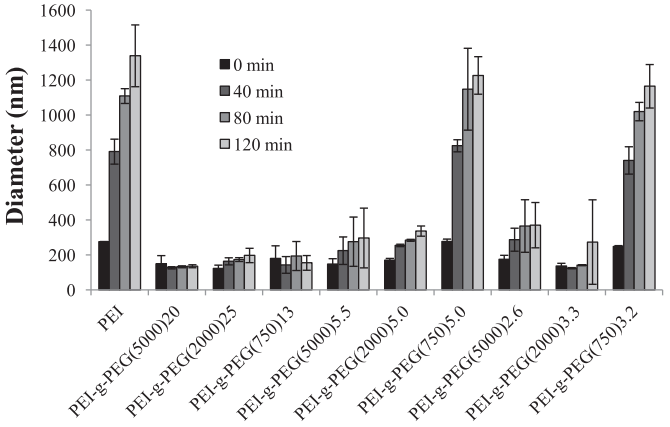

Fig. 9. Polyplex (N/P = 6) hydrodynamic diameter as a function of time in phosphate buffered saline, as measured with dynamic light scattering.

Interestingly, there is no correlation between the results of EMSA and EBEA (Supplemental Information Fig. S5). As stated above, this is likely due to the indirect nature of the assays and serves as further evidence of the care with which one should interpret DNA affinity based on these two common methods.

Isothermal titration calorimetry is a very sensitive technique for simultaneously obtaining the equilibrium constant, enthalpy and stoichiometry of a binding event. Recently, isothermal titration calorimetry (ITC) has been used to determine the thermodynamics of the DNA or siRNA interactions of PEI, poly-L-lysine, poly(2-(dimethylamino) ethyl methacrylate), poly(2-(diethylamino)ethyl methacrylate), poly (glycoamidoamine) and chitosan [43–54]. The difficulty with application of ITC is that not only binding heat is detected. For example, dilution heats can be significant. Binding-induced aggregation of neutral complexes is common at the end of most titrations and is not incorporated into standard fitting models. Also, polymers with buffering capacity can present significant heat as a result of proton uptake upon binding, which is a function of the ionization enthalpy of the buffer in which the titration is taking place. Each of these contributions to the heat signal must be dealt with properly to obtain meaningful thermodynamic binding data.

Here, we accounted for dilution heats by performing control titrations of polymer into buffer and buffer into DNA (the former matched the steady heat signal at the end of the titrations and the latter was negligible). There are two binding events occurring during our titrations of DNA with PEI copolymers. Bimodal isotherms have been observed for multivalent cations and nucleic acids before and were described as binding and then condensation [21,43,46,50,51,55]. The first, exothermic event, described by K_1, ΔH_1 and n_1, is the electrostatic interaction between protonated PEI amines and the phosphate groups of the DNA backbone. Supportive of this assignment is how this event was demonstrated to be entropy driven (Fig. 7a) as are most polyelectrolyte interactions, which are driven by the release of bound counterions and water upon complexation [54,56–60]. The binding constant we determined for unconjugated PEI ($7.6 \times 10^8\ M^{-1}$) is larger than that reported by Utsuno et al. ($1 \times 10^6\ M^{-1}$), but that study investigated a much smaller 600 Da branched PEI and linear, salmon testes DNA [46]. Such structural differences can significantly affect the thermodynamics of the association. All of the PEGylated PEIs show similar or lower K_1 values compared to unconjugated PEI, reflecting weaker electrostatic interaction with DNA. Increasing PEG molecular weight inhibits DNA binding, as demonstrated by a decrease in K_1 from $9.4 \times 10^8\ M^{-1}$ to $1.6 \times 10^8\ M^{-1}$ to $2.0 \times 10^7\ M^{-1}$ for PEI-*g*-PEG(750)$_{5.0}$, PEI-*g*-PEG(2000)$_{5.0}$ and PEI-*g*-PEG(5000)$_{5.5}$, respectively. We attribute this lower association constant to steric hindrance by the well hydrated, flexible PEG chains. At high overall PEG content, the K_1 values overlap for the different PEG molecular weights, suggesting there is a saturation point where DNA affinity is similarly reduced. This was also seen in the EMSA results

for the highest conjugation ratio series (Table 2). Our ITC results also show that PEG conjugation ratios affect DNA association but to less of an extent than molecular weight. For example, PEI-*g*-PEG(750)$_{5.0}$ has a K_1 of 9.4×10^8 M^{-1}, while PEI-*g*-PEG(750)$_{13}$ showed 4.3×10^6 M^{-1}. Higher conjugation results in lower charge density on the polycations, limiting positive binding cooperativity, which is also supported by the larger N/P stoichiometries found for higher degrees of PEG substitution on the PEI. For the PEG(2000) and PEG(5000) copolymers, however, the effect of degree of substitution is not as clear. Perhaps the role of sterics is dominant here.

Since PEI is known for being a "proton sponge" [16,17] and DNA binding is likely to induce amine pKa shifts, we determined the number of protons taken up on binding for the unconjugated polymer, which comes from the slope of the line relating observed enthalpy to buffer ionization enthalpy (Fig. 8) [61]. This data showed that 28% of the PEI amines became protonated as a result of polymer charge neutralization by DNA phosphates. This fraction is reasonable considering that linear PEI is approximately 50% protonated at physiological pH due to charge repulsion down the chain [62]. As DNA electrostatically binds, this charge repulsion is relieved and the pK_as of nearby amines should rise. A similar 25% increase in the protonation state of linear PEI amines after DNA binding was found by Ziebarth and Wang through Monte Carlo simulations [63]. Our results provide a nice experimental compliment in support of the fact that PEI retains buffering capacity, even in its bound form, which has implications for endosomal escape. The intrinsic binding enthalpy, for which the heat of buffering has been eliminated, was obtained by extrapolating the line to $\Delta H_{ion} = 0$ and was found to be −8.7 kJ/mol. Thus, the interaction is more exothermic than reported in Table 4 and Fig. 7 for HEPES buffer, but the driving force is still entropic release of locally bound water and counterions. Although this protonation study was not performed for the full series of copolymers, the buffer effect is expected to be similar for each, and copolymer protonation is expected upon DNA interaction. The association constants did not change significantly with buffer identity; therefore, the specific buffer ions are not involved in the binding.

The second ITC event is aggregation of neutral polyplexes. This assignment is based on dynamic light scattering titrations of the same solutions (data not shown) and the EMSA results, which show charge neutralization at similar N/P ratios. Choosakoonkriang et al. also saw this aggregation in the ITC experiments with branched PEI and DNA, and therefore, decided not to fit the data to extract thermodynamic parameters for the interaction [21]. The magnitude of K_2 should then reflect the extent of aggregation. As seen in Fig. 6, K_2 is 1–2 orders of magnitude larger for PEI, PEI-*g*-PEG(750)$_{3.2}$ and PEI-*g*-PEG(750)$_{5.0}$ compared to that of the other copolymers. This trend is mirrored by the DLS data showing only PEI, PEI-*g*-PEG(750)$_{3.2}$ and PEI-*g*-PEG(750)$_{5.0}$ polyplexes flocculate in physiological ionic strength PBS (Fig. 9). There is a clear trend of reduced K_2 with increasing PEG molecular weight for the 1:30 and 1:12 feeding ratios. At the highest degree of substitution, polyplex aggregation is so weak that the effects of PEG molecular weight are indistinguishable. An effect of PEG conjugation ratio is also noticed. For the shorter PEG chains (750 and 2000 Da), increasing PEG density on the linear PEI leads to decreased aggregation. All of the PEG(5000) copolymers formed complexes with remarkably similarly low aggregation constants (2.8×10^5, 2.8×10^5 and 2.9×10^5 M^{-1} for PEI-*g*-PEG(5000)$_{2.6}$, PEI-*g*-PEG(5000)$_{5.5}$ and PEI-*g*-PEG(5000)$_{20}$, respectively). Such results indicate that when the PEG chain is long enough, a fewer number of them are needed to sterically hinder flocculation. This aggregation event is endothermic, as was seen with branched PEI–siRNA complexes [45], and entropy driven (Fig. 7b) by the release of polyplex-bound water. Interestingly, ITC is able to detect reduced aggregation of polyplexes when DLS cannot, as indicated by the lower K_2 value for PEI-*g*-PEG(750)$_{3.2}$ and PEI-*g*-PEG(750)$_{5.0}$ compared to unconjugated PEI. Thus, we have identified a more sensitive method of characterizing the colloidal stability of polyplexes. Also, the positive assignment of the nature of the second event occurring in these titration curves is highly informative to those trying to interpret convoluted ITC data in any field of polyelectrolyte interactions.

5. Conclusion

In summary, we have investigated the effect of polyethylene glycol molecular weight and conjugation ratio on the interaction of DNA and linear polyethylenimine. ITC studies revealed quantitative thermodynamic parameters, describing two types of entropy-driven interactions (electrostatic binding and polyplex aggregation). We have found that PEGylation reduces DNA affinity as a function of either grafting characteristic. It is important to point out that common assays for comparing DNA affinity of gene delivery agents (ethidium bromide exclusion and electrophoretic mobility shift assays) demonstrated limitations and were often ineffective at distinguishing subtle differences. Such results should be taken into consideration when performing structure–function relationship studies of these systems. Interestingly, we discovered that there is an optimal molecular weight and conjugation ratio of PEG on PEI to obtain strong DNA association with weak polyplex aggregation, and it is about 3% substitution of PEI amines with PEG(5000) chains. This work helps us understand driving forces of polyplex formation and stability and may lead to the rational design of nonviral delivery vehicles that are more effective in vivo.

Acknowledgements

We would like to thank the University of St. Thomas Department of Chemistry for financial support of this project and Kyle Chamberlain for determining some of the experimental parameters used herein.

Appendix A. Supplementary data

Supplementary data to this article can be found online at http://dx.doi.org/10.1016/j.bpc.2015.04.005.

Table 4
DNA binding thermodynamic parameters.

	$K_1 \times 10^{-7}$ (M^{-1})	ΔH_1 (kJ/mol)	n_1 (N/P)	$K_2 \times 10^{-7}$ (M^{-1})	ΔH_2 (kJ/mol)	n_2 (N/P)
PEI	76 ± 3	−3.1 ± 0.7	0.79 ± 0.09	2.2 ± 0.8	1.4 ± 0.2	0.10 ± 0.00
PEI-*g*-PEG(750)$_{13}$	0.67 ± 0.21	−6.1 ± 1.6	1.7 ± 0.2	0.0044 ± 0.0016	2.1 ± 0.4	0.40 ± 0.22
PEI-*g*-PEG(2000)$_{25}$	0.54 ± 0.11	−3.5 ± 0.9	1.4 ± 0.3	0.014 ± 0.003	1.6 ± 0.4	0.21 ± 0.19
PEI-*g*-PEG(5000)$_{20}$	1.0 ± 0.2	−2.2 ± 0.4	0.52 ± 0.02	0.029 ± 0.023	2.3 ± 0.2	0.11 ± 0.01
PEI-*g*-PEG(750)$_{5.0}$	54 ± 1	−1.1 ± 0.8	0.33 ± 0.10	0.17 ± 0.08	1.4 ± 0.3	0.10 ± 0.00
PEI-*g*-PEG(2000)$_{5.0}$	3.4 ± 0.7	−1.9 ± 0.7	0.70 ± 0.22	0.034 ± 0.019	1.4 ± 0.8	0.20 ± 0.12
PEI-*g*-PEG(5000)$_{5.5}$	2.0 ± 0.9	−1.7 ± 1.3	0.63 ± 0.16	0.028 ± 0.011	1.3 ± 0.9	0.12 ± 0.03
PEI-*g*-PEG(750)$_{3.2}$	14 ± 3	−2.5 ± 0.3	0.75 ± 0.02	0.40 ± 0.17	1.2 ± 0.4	0.10 ± 0.00
PEI-*g*-PEG(2000)$_{3.3}$	1.4 ± 0.1	−4.2 ± 0.2	0.81 ± 0.10	0.092 ± 0.008	2.0 ± 0.3	0.11 ± 0.01
PEI-*g*-PEG(5000)$_{2.6}$	3.3 ± 0.4	−0.54 ± 0.49	0.52 ± 0.04	0.028 ± 0.017	1.6 ± 0.5	0.10 ± 0.01

References

[1] M.R. Knowles, K.W. Hohneker, Z. Zhou, J.C. Olsen, T.L. Noah, P.C. Hu, M.W. Leigh, J.F. Engelhardt, L.J. Edwards, K.R. Jones, M. Grossman, J.M. Wilson, L.G. Johnson, R.C. Boucher, A controlled study of adenoviral vector-mediated gene transfer in the nasal epithelium of patients with cystic fibrosis, N. Engl. J. Med. 333 (1995) 823–831.

[2] N.J. Caplan, E.W. Alton, P.G. Middleton, J.R. Dorin, B.J. Stevenson, X. Gao, S.R. Durham, P.K. Jeffery, M.E. Hodson, C. Coutelle, L. Huang, D. Porteous, R. Williamson, D. Geddes, Liposome-mediated CFTR gene transfer to the nasal epithelium of patients with cystic fibrosis, Nat. Med. 1 (1995) 39–46.

[3] D.J. Porteous, J.R. Dorin, G. McLachlan, H. Davidson-Smith, H. Davidson, B.J. Stevenson, A.D. Carothers, W.A. Wallace, S. Morallee, C. Hoenes, G. Kallmeyer, U. Michaelism, K. Naujoks, L.P. Ho, J.M. Samways, M. Imrie, A.P. Greening, J.A. Innes, Evidence for safety and efficacy of DOTAP cationic liposome mediated CFTR gene transfer to the nasal epithelium of patients with cystic fibrosis, Gene Ther. 3 (1997) 210–218.

[4] D.R. Gill, K.W. Southern, K.A. Mofford, T. Seddon, L. Huang, F. Sorgi, A. Thompson, L.J. MacVinish, R. Ratcliff, D. Bilton, D.J. Lane, J.M. Littlewood, A.K. Webb, P.G. Middleton, W.H. Colledge, A.W. Cuthbert, M.J. Evans, C.F. Higgins, S.C. Hyde, A placebo controlled study of liposome mediated gene transfer to the nasal epithelium of patients with cystic fibrosis, Gene Ther. 4 (1997) 199–209.

[5] G.J. Nabel, E.G. Nabel, Z.Y. Yang, B.A. Fox, G.E. Plautz, X. Gao, L. Huang, S. Shu, D. Gordon, A.E. Change, Direct gene transfer with DNA–liposome complexes in melanoma: expression, biological activity and lack of toxicity in humans, Proc. Natl. Acad. Sci. U. S. A. 90 (1993) 11307–11311.

[6] J. Rubin, E. Galanis, H.C. Pitot, R.L. Richardson, P.A. Burch, J.W. Charboneau, C.C. Reading, B.D. Lewis, S. Stahl, E.T. Akporiaye, D.T. Harris, Phase I study of immunotherapy of hepatic metastases of colorectal carcinoma by direct gene transfer of an allogeneic histocompatibility antigen, HLA-B7, Gene Ther. 4 (1997) 419–425.

[7] N.J. Vogelzang, T.M. Lestingi, G. Sudakoff, S.A. Kradjian, Phase I study of immunotherapy of metastatic renal cell carcinoma by direct gene transfer into metastatic lesions, Hum. Gene Ther. 5 (1994) 1357–1370.

[8] N.J. Vogelzang, G. Sudakoff, E.M. Hersh, Clinical experience in phase I and phase II testing of direct intratumoral administration with allovectin-7: a gene-based immunotherapeutic agent, Proc. Am. Soc. Clin. Oncol. 15 (1996) 235.

[9] O. Boussif, F. Lezoualc'h, M.A. Zanta, M.D. Mergny, D. Scherman, B. Demeneix, J.P. Behr, A versatile vector for gene and oligonucleotide transfer into cells in culture and in vivo: polyethylenimine, Proc. Natl. Acad. Sci. U. S. A. 16 (1995) 7297–7301.

[10] M. Ohsake, T. Okuda, A. Wada, T. Hirayama, T. Niidome, H. Aoyagi, In vitro gene transfection using dendritic poly(L-lysine), Bioconjug. Chem. 13 (2002) 510–517.

[11] J.F. Kukowska-Latallo, A.U. Bielinska, J. Johnson, R. Spindler, D.A. Tomalia, J.R. Baker, Efficient transfer of genetic material into mammalian cells using starburst polyamidoamine dendrimers, Proc. Natl. Acad. Sci. U. S. A. 93 (1996) 4897–4902.

[12] Y. Zhang, A. Satterlee, L. Huang, In vivo gene delivery by nonviral vectors: overcoming hurdles? Mol. Ther. 20 (2012) 1298–1304.

[13] W.T. Godbey, K.K. Wu, A.G. Mikos, Poly(ethylenimine) and its role in gene delivery, J. Control. Release 60 (1999) 149–160.

[14] U. Lungwitz, M. Breunig, T. Blunk, A. Gopferich, Polyethylenimine-based non-viral gene delivery systems, Eur. J. Pharm. Biopharm. 60 (2005) 247–266.

[15] M. Neu, D. Fischer, T. Kissel, Recent advances in rational gene transfer vector design based on poly(ethyleneimine) and its derivatives, J. Gene Med. 7 (2005) 992–1009.

[16] J.P. Behr, The proton sponge: a trick to enter cells the viruses did not exploit, Chimia 51 (1997) 34–36.

[17] N.D. Sonawane, F.C. Szoka, A.S. Verkman, Chloride accumulation and swelling in endosomes enhances DNA transfer by polyamine–DNA polyplexes, J. Biol. Chem. 278 (2003) 268–275.

[18] A. Beyerle, O. Merkel, T. Stoeger, T. Kissel, PEGylation affects cytotoxicity and cell-compatibility of poly(ethylene imine) for lung application: structure function relationships, Toxicol. Appl. Pharmacol. 242 (2010) 146–154.

[19] D. Fischer, T. Bieber, Y. Li, H.P. Elsasser, T. Kissel, A novel non-viral vector for DNA delivery based on low molecular weight, branched polyethylenimine: effect of molecular weight on transfection efficiency and cytotoxicity, Pharm. Res. 16 (1999) 1273–1279.

[20] P.R. Leroueil, S. Hong, A. Mecke, J.R. Baker Jr., B.G. Orr, M.M. Banaszak Holl, Nanoparticle interaction with biological membranes: does nanotechnology present a janus face? Acc. Chem. Res. 40 (2007) 335–342.

[21] S. Choosakoonkriang, B.A. Lobo, G.S. Koe, C.R. Middaugh, Biophysical characterization of PEI/DNA complexes, J. Pharm. Sci. 92 (2003) 1710–1722.

[22] L. Wightman, R. Kircheis, V. Rossler, S. Carotta, R. Ruzicka, M. Kursa, E. Wagner, Different behavior of branched and linear polyethylenimine for gene delivery in vitro and in vivo, J. Gene Med. 3 (2001) 362–372.

[23] S.J. Sung, S.H. Min, K.Y. Cho, S. Lee, Y.J. Min, Y.I. Yeom, J.K. Park, Effect of polyethylene glycol on gene delivery of polyethyleneimine, Biol. Pharm. Bull. 26 (2003) 492–500.

[24] W.C. Tseng, T.Y. Fang, L.Y. Su, C.H. Tang, Dependence of transgene expression and the relative buffering capacity of dextran-grafted polyethyleneimine, Mol. Pharm. 2 (2005) 224–232.

[25] M. Ogris, S. Brunner, S. Schüller, R. Kircheis, E. Wagner, A PEGylated DNA/transferrin-PEI complexes: reduced interaction with blood components, extended circulation in blood and potential for systemic gene delivery, Nature 6 (1999) 595–605.

[26] M.R. Park, K.O. Han, I.K. Han, M.H. Cho, J.W. Nah, Y.J. Choi, C.S. Cho, Degradable polyethylenimine-alt-poly(ethylene glycol) copolymers as novel gene carriers, J. Control. Release 105 (2005) 367–380.

[27] T. Merdan, K. Kunath, H. Petersen, U. Bakowsky, K.H. Voigt, J. Kopecek, T. Kissel, PEGylation of poly(ethylene imine) affects stability of complexes with plasmid DNA under in vivo conditions in a dose-dependent manner after intravenous injection into mice, Bioconjug. Chem. 16 (2005) 785–792.

[28] H. Petersen, K. Kunath, A.L. Martin, S. Stolnik, C.J. Roberts, M.C. Davies, T. Kissel, Star-shaped poly (ethylene glycol)-block-polyethylenimine copolymers enhance DNA condensation of low molecular weight polyethyleneimines, Biomacromolecules 3 (2002) 926–936.

[29] P. Banerjee, R. Weissleder, A. Bogdanov Jr., Linear polyethyleneimine grafted to a hyperbranched poly(ethylene glycol)-like core: a copolymer for gene delivery, Bioconjug. Chem. 17 (2006) 125–131.

[30] C.H. Ahn, S.Y. Chae, Y.H. Bae, S.W. Kim, Biodegradable poly(ethylenimine) for plasmid DNA delivery, J. Control. Release 80 (2002) 273–282.

[31] H. Peterson, P.M. Fechner, A.L. Martin, K. Kunath, S. Stolnik, C.J. Roberts, D. Fischer, M.C. Davies, T. Kissel, Polyethyleneimine-graft-poly(ethylene glycol) copolymers: influence of copolymer block structure on DNA complexation and biological activities as gene delivery system, Bioconjug. Chem. 13 (2002) 845–854.

[32] X. Luo, S. Pan, M. Feng, Y. Wen, W. Zhang, Stability of poly(ethylene glycol)-graft-polyethyleneimine copolymer/DNA complexes: influences of PEG molecular weight and PEGylation degree, J. Mater. Sci. Mater. Med. 21 (2010) 597–607.

[33] G.P. Tang, J.M. Zend, S.J. Gao, Y.X. Ma, L. Shi, Y. Li, H.P. Too, S. Wang, Polyethylene glycol modified polyethylenimine for improved CNS gene transfer: effects of PEGylation extent, Biomaterials 24 (2003) 2351–2362.

[34] X. Zhang, S.R. Pan, H.M. Hu, G.F. Wu, M. Feng, W. Zhang, X. Luo, Poly(ethylene glycol)-block-polyethylenimine copolymers as carriers for gene delivery: effects of PEG molecular weight and PEGylation degree, J. Biomed.Mater. Res. Part A 84 (2008) 795–804.

[35] M.L. Read, T. Bettinger, D. Oupicky, Methods for studying the formation of polycation–DNA complexes and properties useful for gene delivery, Methods Mol. Med. 65 (2001) 131–148.

[36] R.N. Goldberg, N. Kishore, R.M. Lennen, Thermodynamics quantities for the ionization reactions of buffers, J. Phys. Chem. Ref. Data 31 (2002) 231–370.

[37] R.E. Fitzsimmons, H. Uludag, Specific effects of PEGylation on gene delivery efficacy of polyethylenimine: interplay between PEG substitution and N/P ratio, Acta Biomater. 8 (2012) 3941–3955.

[38] G. Maurstad, B.T. Stokke, K.M. Varum, S.P. Strand, PEGylated chitosan complexes DNA while improving polyplex colloidal stability and gene transfection efficiency, Carbohydr. Polym. 94 (2013) 436–443.

[39] R.L. Jones, A.C. Lanier, R.A. Keel, W.D. Wilson, The effect of ionic strength on DNA-ligand unwinding angles for acridine and quinolone derivatives, Nucleic Acids Res. 8 (1980) 1613.

[40] J.G. Wang, The degree of unwinding of the DNA helix by ethidium. I. titration of twisted PM2 DNA molecules in alkaline cesium chloride density gradients, J. Mol. Biol. 89 (1974) 783–801.

[41] H.M. Sobell, C. Tsai, S.C. Jain, S.G. Gilbert, Visualization of drug nucleic acid interactions at atomic resolution. III. Unifying structural concepts in understanding drug–DNA interactions and their broader implications in understanding protein–DNA interactions, J. Mol. Biol. 114 (1977) 333–365.

[42] K. Fant, E.K. Esbjorner, A. Jenkins, M.C. Grossel, P. Lincoln, B. Norden, Effects of PEGylation and acetylation of PAMAM dendrimers on DNA binding, cytotoxicity and in citro transfection efficiency, Mol. Pharm. 7 (2010) 1734–1746.

[43] T. Ehtezazi, U. Rungsardthong, S. Stolnik, Thermodynamic analysis of polycation–DNA interaction applying titration microcalorimetry, Langmuir 19 (2003) 9387–9394.

[44] U. Rungsardthong, T. Ehtezazi, L. Bailey, S.P. Armes, M.C. Garnett, S. Stolnik, Effect of polymer ionization on the interaction with DNA in nonviral gene delivery systems, Biomacromolecules 4 (2003) 683–690.

[45] M. Zheng, G.M. Pavan, M. Neeb, A.K. Schaper, A. Danani, G. Klebe, O.M. Merkel, T. Kissel, Targeting the blind spot of polycationic nanocarrier-based siRNA delivery, ACS Nano 6 (2012) 9447–9454.

[46] K. Utsuno, H. Uludag, Thermodynamics of polyethylenimine–DNA binding and DNA condensation, Biophys. J. 99 (2010) 201–207.

[47] T. Bronich, A.V. Kabanov, L.A. Marky, A thermodynamic characterization of the interaction of a cationic copolymer with DNA, J. Phys. Chem. B 105 (2001) 6042–6050.

[48] W. Kim, Y. Yamasaki, K. Kataoka, Development of a fitting model suitable for the isothermal titration calorimetric curve of DNA with cationic ligands, J. Phys. Chem. B 110 (2006) 10919–10925.

[49] J.F. Tan, H.P. Too, T.A. Hatton, K.C. Tam, Aggregation behavior and thermodynamics of binding between polyethylene oxide-block-poly(2-(diethylamino)ethyl methacrylate) and plasmid DNA, Langmuir 22 (2006) 3744–3750.

[50] L.E. Prevette, T.E. Kodger, T.M. Reineke, M.L. Lynch, Deciphering the role of hydrogen bonding in enhancing pDNA–polycation interactions, Langmuir 23 (2007) 9773–9784.

[51] L.E. Prevette, M.L. Lynch, K. Kizjakina, T.M. Reineke, Correlation of amine number and pDNA binding mechanism for trehalose-based polycations, Langmuir 24 (2008) 8090–8101.

[52] D. Huang, N. Korolev, K. Eom, J. Tam, L. Nordenskiold, Design and biophysical characterization of novel polycationic e-peptides for DNA compaction and delivery, Biomacromolecules 9 (2008) 321–330.

[53] M. Yin, K. Ding, R. Gropeanu, J. Shen, R. Berger, T. Weil, K. Mullen, Dendritic star polymers for efficient DNA binding and stimulus-dependent DNA release, Biomacromolecules 9 (2008) 3231–3238.

[54] P. Ma, M. Lavertu, F. Winnik, M. Buschmann, New insights into chitosan–DNA interactions using isothermal titration microcalorimetry, Biomacromolecules 10 (2009) 1490–1499.

[55] M.M. Patel, T.J. Anchordoquy, Contribution of hydrophobicity to thermodynamics of ligand-DNA binding and DNA collapse, Biophys. J. 88 (2005) 2089–2103.

[56] C.K. Nisha, S.V. Manorama, M. Ganguli, S. Maiti, J.N. Kizhakkedathu, Complexes of poly(ethylene glycol)-based cationic random copolymer and calf thymus DNA: a complete biophysical characterization, Langmuir 20 (2004) 2386–2396.

[57] Y.L. Zhou, Y.Z. Li, The interaction of poly(ethylenimine) with nucleic acids and its use in determination of nucleic acids based on light scattering, Spectrochim. Acta Part A 60 (2004) 377–384.
[58] G.S. Manning, Limiting laws and counterion condensation in polyelectrolyte solutions, J. Chem. Phys. 51 (1969) 924–933.
[59] G.S. Manning, The molecular theory of polyelectrolyte solutions with applications to the electrostatic properties of polynucleotides, Q. Rev. Biophys. 11 (1978) 179–246.
[60] V. Ball, C. Maechling, Isothermal microcalorimetry to investigate non specific interactions in biophysical chemistry, Int. J. Mol. Sci. 10 (2009) 3283–3315.
[61] B.M. Baker, K.P. Murphy, Evaluation of linked protonation effects in protein binding reactions using isothermal titration calorimetry, Biophys. J. 71 (1996) 2049–2055.
[62] R.G. Smits, G.J.M. Koper, M. Mandel, The influence of nearest- and next-nearest-neighbor interactions on the potentiometric titration of linear poly(ethylenimine), J. Phys. Chem. 97 (1993) 5745–5751.
[63] J.D. Ziebarth, Y. Wang, Understanding the protonation behavior of linear polyethylenimine in solutions through Monte Carlo simulations, Biomacromolecules 11 (2010) 29–38.